

Radiation Field in the Vicinity of the Collider Center

A. J. Stevens

October 1994

Collider Accelerator Department
Brookhaven National Laboratory

U.S. Department of Energy

USDOE Office of Science (SC)

Notice: This technical note has been authored by employees of Brookhaven Science Associates, LLC under Contract No. DE-AC02-76CH00016 with the U.S. Department of Energy. The publisher by accepting the technical note for publication acknowledges that the United States Government retains a non-exclusive, paid-up, irrevocable, world-wide license to publish or reproduce the published form of this technical note, or allow others to do so, for United States Government purposes.

DISCLAIMER

This report was prepared as an account of work sponsored by an agency of the United States Government. Neither the United States Government nor any agency thereof, nor any of their employees, nor any of their contractors, subcontractors, or their employees, makes any warranty, express or implied, or assumes any legal liability or responsibility for the accuracy, completeness, or any third party's use or the results of such use of any information, apparatus, product, or process disclosed, or represents that its use would not infringe privately owned rights. Reference herein to any specific commercial product, process, or service by trade name, trademark, manufacturer, or otherwise, does not necessarily constitute or imply its endorsement, recommendation, or favoring by the United States Government or any agency thereof or its contractors or subcontractors. The views and opinions of authors expressed herein do not necessarily state or reflect those of the United States Government or any agency thereof.

AD/RHIC/RD-77

RHIC PROJECT
Brookhaven National Laboratory

Radiation Field in the Vicinity of the Collider Center

A. J. Stevens

October 1994

Radiation Field in the Vicinity of the Collider Center

I. Introduction

The Collider Center and the adjoining cryogenic support building (Bldg. 1005S) are unique among the buildings close to the collider tunnel because these are locations where the occupancy by non-radiation workers is high.¹ The criteria which has been adopted for such regions is very stringent, namely;

$$\begin{aligned} &< 15 \text{ mrem/yr from normal losses and} \\ &< 10 \text{ mrem from design basis fault} \end{aligned}$$

where the design basis fault in this case² is loss of half of the full energy, full intensity beam on a single nearby magnet.

This note describes calculations of the dose equivalent from local beam loss at both the nearest point of these buildings to the collider ring and on the berm in the vicinity of these buildings. The berm itself is considered to be a point of low occupancy. For such regions the criteria are 16 times the numbers above¹ or:

$$\begin{aligned} &< 240 \text{ mrem/yr from normal losses and} \\ &< 160 \text{ mrem from design basis fault} \end{aligned}$$

Regions not in conformance with these criteria must be controlled (restricted to occupancy by radiation workers) or have appropriate physical barriers to prevent access.

II. Existing Topology

The topological map of existing berm elevation contours³ in this region of the tunnel is shown as Fig. 1. Fig. 2 shows a half cross section (on the building side of the tunnel) at the point labeled A-A' in Fig. 1. The berm at this point is "typical" in the sense that it conforms to the vertical berm thickness of ~ 19 ft. of earth originally specified⁴ to be present in the vicinity of the collider center. However, the drop of the berm to the ~ 90 ft elevation in Fig. 1, while still adjacent to Bldg. 1005, is not as specified. This is more important on the collider center side of Bldg 1005 than on the cryogenic support side because the latter section of the building has only a ground floor. As should be evident from the "typical" cross section shown in Fig. 2, the ground floor is far better protected than higher elevations. The smallest thickness of soil shielding along a line directed toward the collider center is ~ 16.5 ft. as shown by the dashed line in Fig. 2.

Fig. 3 shows the half cross section of section labeled B-B' in Fig. 1. This location is one of several which differ significantly from the "typical" case shown in Fig. 2. The first problem is

that the ceiling height is at elevation 83.5 ft. instead of the 76 ft. of Fig. 2. Secondly, an equipment alcove exists here which represents a considerable "hole" in the transverse shielding. Finally, a small (4.5 inch diameter) cryogenics return line penetration exists. Note that one point exists with only ~ 7 ft. of berm thickness. The length of the penetration as determined from Fig. 3 would be $32.5 - 17.5 = 15$ ft. which compares to a measured length of 14 ft.

The position of the "first leg" of the main access labyrinth connecting Bldg. 1005 to the collider tunnel is indicated by the position D-D' in Fig. 1. The cross section for this location will be shown and discussed in more detail in section IV below.

The other cross sections which differ significantly from Fig. 2 are those where additional penetrations exist. In total, there are five penetrations in the berm in the vicinity of Bldg. 1005. These are the cryo return line shown in Fig. 3, the two vents shown in Fig. 1, the escape shaft indicated there also, and the main access labyrinth. The estimate of dose equivalent at the exits of these penetrations is amenable to analysis by traditional labyrinth formula supplemented by an estimate of punch-through which comes from the walls of the last leg of each penetration. This estimate will be described in section VI below.

III. Method

For direct radiation, the dose equivalent is estimated by utilizing CASIM⁵ calculations. Many of the estimates made in the following sections are scaled from a simple cylindrically symmetric geometry with magnets in a tunnel of radius 2.5m. Only soil and a series of magnets corresponding to the layout of the regular lattice are assumed to be present. The approximation of the magnets is as follows:

Radius (cm)	Material
$r < 3.645$	vacuum
$3.645 < r < 4.00$	Beam pipe Fe with density reduced to 3.62 g/cc
$4.00 < r < 13$	Yoke Fe with full density (7.8 g/cc)
$r < 39$	Cryostat Fe with density reduced to .15 (~2%)

The beam pipe is exaggerated in thickness (but reduced in density) to reduce the likelihood of "stepping over" the pipe during transport. The lattice is described by Quad, Drift, Dipole, Drift, Quad...with lengths of 1.13m for the quads, 9.45m for the dipoles, and 2.12m for the drift regions where only the beam pipe is present. The actual presence of magnetic fields and a second ring in the tunnel are ignored. Other deep penetration calculations have shown that the effect of the magnetic field is small.⁶

The beam is always assumed to be lost in a "scraping mode" over the length of one of the ~ 1 m quads. This is simulated by forcing an interaction midway through the beam pipe in the transverse direction and uniformly along the quadrupole length.

Fig 4 shows the results of the CASIM calculation in this simple geometry.⁷ The quantity plotted is the square of the transverse distance times the star density. The open circles are for 250 GeV/c protons. For comparison, the filled circles represent the star density per Au ion divided by 100. There are 100 times less Au ions in the beam than protons. This scaling happens to be within 5% of the scaling of loss per nucleon.⁸ The $\sim 10\%$ higher star density for Au ions shown in Fig.4 is a real effect which simply reflects the neutron content of the Au ions, but it is an artifact of the calculation which forces an ion to interact without losing energy between the time that the beam pipe is encountered and the time that the ion interacts. This effect is negligible for protons, but larger than (and in the opposite direction from) the 10% effect in Fig. 4 for Au ions whose ionization energy loss is quite large. It is therefore sufficient to consider only the 250 GeV/c protons. As shown in Fig. 4, a reasonable approximation for the maximum star density is:

$$\text{Star Density (stars/cc-proton)} = 6.6 \times 10^{-6} \times \frac{e^{-d/1.67}}{R^2}$$

where R is the transverse distance and d the soil thickness in meters. The coefficient does not take credit for the concrete wall in the tunnel in the vicinity of Bldg. 1005. A conservative allowance for this effect is to simply substitute 1 ft. of concrete for 1 ft. of soil which reduces the coefficient to 5.7×10^{-6} . This expression — with either of the two coefficients as appropriate and various reduction factors as explained below — will be used repeatedly in the subsequent evaluations.

The star density to dose equivalent conversion factor is taken as *twice* the normal factor to conservatively allow for the recommendation⁹ that low energy neutrons have their quality factor doubled for design purposes. For BNL soil, the doubled factor is 2.4×10^{-5} rem/star/cc.

IV. Faults

The only source of "normal loss" near the collider center is beam-gas interactions which, for completeness, are analyzed in the next section. However, this loss will be shown to be small. In practice, the shielding must be designed for the possibility of the faults mentioned above.² The dose at penetration exits from nearby faults will be treated in section VI below. In this section the results of the fault dose estimation in other locations are reported.

IV.A Dose Equivalent in Regions With Complete Berm.

As mentioned above, the cross section shown in Fig. 2 was as originally specified. At the edge of the berm, the dashed line shown in Fig. 2 has $R = 26$ ft = 7.92m and $D = 16.5$ ft. = 5.029m. Evaluating the expression in the section above gives 1.20×10^{-15} rem/p. Half the design

intensity is 2.85×10^{12} protons which gives 3.42 mrem on the berm top. Taking a conservative 1/R fall off to the edge of the collider center gives 1.24 mrem at the edge of the building. These numbers are well within the design criteria, even at 4 times the design intensity.

As remarked above, the fall off of the berm elevation contours in the northeast direction in Fig. 1 represents a potential problem. Fig. 5 shows a cross section at a point just northeast of C-C' in Fig. 1 — just to the northeast of the vent headed toward the closest corner of the collider center. At this point, the tunnel cross section has "returned" to that used in the original CASIM calculation. Using the same method of estimation as above along the ray shown gives 14 mrem per 2.85×10^{12} proton fault at the berm and 4.5 mrem at the edge of the building. **At 4 times the design intensity, the dose equivalent at the building does not meet the high occupancy requirement;** approximately 3 ft. of additional berm is required. The dashed line shown above the existing berm in Fig. 5 is basically an extension of the elevation contour at A-A' in the transverse distance range 12-28 ft., although somewhat lower than A-A' on the berm top. This is slightly more than is needed for this spot alone, but will also help with the vent along the C-C' line which is discussed in section VI below.

IV.B Dose Equivalent in Thinly Shielded Regions

IV.B.1 Region Near the Equipment Alcove

The estimate of the dose equivalent in the thinly shielded region shown in Fig. 3 is complicated by the fact that this region extends for only 21.5 feet along the beam direction. The implication of this fact is that the dose on the berm will be reduced somewhat from what would be obtained by applying the formula given in section III directly. Fig. 6 shows the same cross section as Fig. 3 with two lines drawn indicating points of minimal transverse shielding. In order to estimate the reduction from the finite length of the enclosure, a series of CASIM calculations were done where the material shown in Fig. 6 is symmetrized around the line shown drawn to the back of the alcove. This geometry is shown in Fig. 7.¹⁰ Note also a part of the first leg of the escape shaft shown in Fig. 1 is indicated in this figure. In such a geometry, the worst case location of loss is not known a priori, so several runs were made changing the magnet locations relative to the alcove beam line position. The reduction factor was determined to be a factor of 1.8

Fig. 8 shows the estimated dose per proton on the top of the berm as a function of transverse distance at the B-B' location (Fig. 3 or Fig. 6) derived from the expression in section III reduced by 1.8. For the canonical fault of 2.85×10^{12} protons, the "hot spot" in Fig. 8 at 18.8 ft. in the transverse direction is 151 mrem. This is barely within the criteria of 160 mrem at the design intensity discussed in section I, but *is not within the criteria at 4 times the design intensity.*

The other problem to be considered is the radiation in the local high occupancy areas. Fig. 9 is another re-run of Fig. 3 showing a 6 ft. tall stick figure in the cryogenics support building. The ray going through the hot spot is well above the high occupancy section (only a ground floor exists) of this building. If the ray headed toward the 83' elevation at the edge of the building is

taken as providing a reasonable margin of safety, the fault dose at the edge of the building, again taking a 1/R fall off between the berm and the edge of the building, becomes ~ 1.7 mrem at design intensity. The limiting problem in this region is therefore the low occupancy region on the berm.

For the 4 times design intensity more shielding is needed in this region. Fig. 9 also shows crosses which represent the addition of 3 vertical feet of earth over much of the berm. The contour shown provides an additional 3.5 ft. of earth at the "hot spot" shown in Fig. 8. With this addition, the berm would be well below the 160 mrem criteria at 4 times the design intensity and a margin of safety would be present in the high occupancy region. The additional cover must begin on the northeast side of the escape shaft shown in Fig. 1 and extend ~ 50 ft.

IV.B.2: Region Near the Main Access Labyrinth.

The other problem area is the main access labyrinth. The position of the first leg is indicated by D-D' in Fig. 1. The cross section at this point is shown in Fig. 10. This figure shows about 9 ft. of earth between the end of the first leg and the wall of the Collider Center. However, the length of this penetration is only 8 ft. A CASIM calculation was once again performed similar to those done in the alcove region. In this case the reduction factor relative to the unrestricted length calculation was found to be 3.8. The dose equivalent at the wall for the design intensity fault of 2.85×10^{12} protons is 8.2 mrem. Again, although nominally within the criteria at design intensity, a problem exists at higher beam levels. Unlike the region near the equipment alcove, more earth cannot be added here. The solution here is either to bury steel in the ground or, more simply, to place a concrete block at the end of the first leg. The 8 ft. width is more than required for access and a 3 ft. thick concrete block provides a sufficient reduction factor for 4 times design intensity.

IV.C *Consideration of the Opposite Berm Side*

The side of the berm opposite the Collider Center will not be discussed in detail. A casual inspection of Fig. 1 shows that the elevation contours on the opposite side extend farther in the transverse direction from the tunnel center line and therefore more earth is present. There is, for example, a "hot spot" corresponding to that indicated in Fig. 3 on the opposite side, but an additional 3 ft. of earth is present here which is enough to satisfy the 4 times day-1 intensity criteria. The one penetration on this side will be discussed in section VI below.

V. Beam Gas

As mentioned in the introduction, the only source of normal loss near Bldg. 1005 is beam-gas interactions in the cold section of the collider. The specification for the **maximum** vacuum in the cold regions is expected to be 10^{-11} Torr.¹¹ At a given point, the interaction rate is given by:

$$Interactions/cm \cdot sec = I_0 \times n \times \sigma$$

where I_0 is the circulating beam (particles/sec), n the number density, and σ the interaction cross section. The number density is given by:

$$n = 6.656 \times 10^{18} \frac{P}{T} \text{ molecules / cm}^3$$

where P is the pressure in Torr and T is the temperature. At 10^{-11} Torr and 4°K , $n=2.414 \times 10^7$. In the cold section, the gas is essentially hydrogen.¹² First consider a proton beam with a cross section of 45 mb. The interaction rate multiplied by 2 to account for both beams illuminating a given point is then:

$$Interactions/cm \cdot sec = 2 \times \frac{5.7 \times 10^{12}}{12.6 \times 10^{-6}} \times 2.414 \times 10^7 \times 45 \times 10^{-27} = .983 \text{ Int / cm} \cdot \text{sec}$$

where there are less than or equal to 5.7×10^{12} protons circulating with a 12.6 μsec . period. For Au beams, the corresponding number is .322 interactions/cm per sec.¹³

At a given observation point outside the berm, the dose equivalent per year is given by:

$$rem / year = I \times C \times T \times \int_z S.D. dz$$

where I is the interaction rate computed above, C is the star density to rem conversion constant, (2.4×10^{-5} as given in section III above) T is the seconds per year in a given mode, and $S.D.$ is the CASIM star density at the observation point from an interaction a distance z away. The values of T come from the Beam Loss Scenario² which makes allowance for 8 weeks of p,Au running and 26 weeks of Au, Au running. This gives (given that the presence of 2 beams was accounted for in the expression for I) 1.814×10^7 seconds per year with an Au beam and 2.419×10^6 seconds per year with protons.

Before proceeding further, a digression is required. In section III above, it was observed that the star density produced for fault situations (Au or protons on Fe) scaled between protons and Au ions; which is to say that the identical maximum star density is obtained if one scales by the number of nucleons and the energy per nucleon to the 0.8 power. Physically, this means that — when viewed from a distance — each nucleon in the Au nucleus interacts with an Fe nucleus. Now in a single interaction this is most unlikely to happen: typically only a part of the nucleons interact with the Fe nucleus while a part of the incident Au nucleus gets sheared off. However, this forward going fragment encounters another Fe nucleus in the beam pipe etc., so that when viewed from even a small distance away, all the Au nucleons appear to have interacted at a point.

This is certainly not the case for Au, proton collisions in the center of the vacuum chamber. In most collisions one expects that forward fragments will go a long way. To simulate

this process in detail would require an accurate knowledge of the fragmentation process and the tracking (perhaps even multi-turn tracking!) of fragments through the entire lattice. *We therefore continue to make the assumption that every Au interaction at a point involves every nucleon.* At first blush this would seem to vastly overestimate the contribution at a point of observation because the maximum star density is in fact much lower at any specific point from an interaction at any other specific point than will be assumed. However, to first order this is compensated for by the fact that, in reality, the integral over the z direction should encompass the entire machine if the process could be simulated exactly. To second order however, *the approximation is an over-estimate* because many fragments which originate a long way from the collider will be intercepted by a limiting aperture collimator which exists for that purpose. We therefore make the simplifying assumption, expected to overestimate the beam-gas radiation, that:

$$S.D.(Au) = 197 \times \left(\frac{100}{250} \right)^{0.8} \times S.D.(p)$$

One can now plug in the numbers for I,C, and T which gives:

$$rem / year = 1.33 \times 10^4 \times \int S.D.(p) dz$$

Fig. 11 shows a star density plot at a "typical" depth and radius in a tunnel geometry. We assume this shape at any depth and scale the curve by the usual $\exp(-d/.67)/R^2$ for any radius and soil depth. A small FORTRAN program readily performs the integral numerically. At a point on the berm shown in Fig. 2, which corresponds to the berm cross section at A-A' in Fig. 1, the result turns out to be 0.37 mrem/year. **This is 1 order of magnitude below the fault at the same location calculated in the previous section.** Given the rather optimistic projection of circulating beam per year, the fact that no credit for the decrease in beam intensity as a function of time has been taken, and the fact that, as mentioned above, many of the Au-gas fragments are expected to be collimated, this estimate is likely to be highly exaggerated.

VI. Penetrations

As mentioned above, five penetrations exist in the berm in this region: 2 vents, an access labyrinth, an escape shaft, and a small cryogenic return line. In this section, estimates of the *excess* dose equivalent emerging from these "holes" are made. With the exception of the cryogenics return line, which is a straight penetration, the penetrations are multi-legged. These have been analyzed by Gollon¹⁴, and the bulk of this section relies on this analysis, although some adjustment of the parameters assumed in Ref. [14] is required. The "bottom line" of the estimates which follow is that the penetrations, as such, do not appear to cause problems.

VI.A Vent at C-C'.

The first penetration considered is the vent along the C-C' line in Fig. 1, whose cross section is shown in Fig. 12. As mentioned above, this region is thinly shielded even in the absence of penetrations, and it will be recommended that additional earth be added as indicated in Fig. 5. This means that this vent shaft must be extended such that the center of the 2 ft. radius shaft emerges at the 88.5 ft. elevation as shown in Fig. 12.

In Ref. [14] this penetration is Type V-7. However, the second leg is considerably longer than assumed. Specifically, in units of the square root of the area of the opening ($\sqrt{\pi 2 \text{ ft.}^2}$) the leg2 length in Ref [14] is 5.15 instead of the 3.95 assumed there. I have chosen the second (and subsequent) leg attenuation factor of Goebel to scale Gollon's result. This attenuation is:

$$H = \frac{1}{1 + 2.8 \times d \times 1.57^{d+2}}$$

where d is the leg length expressed as indicated here. The reduction factor is .448 which converts Gollon's estimate of 201 mrem for a fault of half the beam at 4 times design intensity to 90 mrem. This represents the excess dose at the point where the center of the penetration emerges from the berm.

As it happens in this case, the total recommended additional earth cover along the ray in Fig. 5 achieves a reduction in the direct dose of a factor of ~ 10 from the value calculated in section IV (A) above. At 4 times design intensity, the direct dose is therefore only about 5 mrem so that the total dose, 90 mrem + 5 mrem, is below the low occupancy criteria. However, this is **not** a general requirement since the vents will be covered and can be designated as potential radiation hazards. A quantity of interest therefore is the dose that a person standing **beside** an emerging vent shaft might receive.

First, consider a very crude estimate. If a 6 ft. tall person would be standing 1 ft. outside of the 2 ft. radius vent under consideration, then the center of the person's body would be about 4.24 ft. from the center of the exit point. If the dose were treated as uniformly emerging from this single point into a 2π solid angle then the reduction at the center of the body would be

$$\frac{4\pi}{2\pi} \times \frac{1}{4.24^2} \approx 0.1$$

where the 4π in the numerator is the area of the opening in this particular case. Now in fact, the emerging dose is directional. Fig. 13 shows a plot of a CERN calculation¹⁵ of neutron direction with respect to a labyrinth axis for two different values of the length, again expressed in the "universal" units of the square root of the area. The increased forward directionality as a function of length is clear. In the case of the vent considered here, $d = 5.15$ which would be more forward peaked than the cases plotted. This forward peaking clearly reduces the dose to the hypothetical individual standing beside the vent. Based on the reasoning presented here, it will be **assumed** that an order of magnitude reduction factor always exists between the dose calculated at the center of the berm exit of a vent and a person standing beside the vent.

Returning to Fig. 12, an estimate must be made for the emerging dose at the Collider Center whose floor levels are shown as dashed lines in the drawing. It is clear that all the floors are at angle which is greater than 45° from the axis of the vent second leg. If one ignores the backwards (>90°) angles in Fig. 13 entirely and sums the dashed curves which severely underestimates the forward directionality in this case, the fraction of neutrons between 45 and 90°, a solid angle of 4.44 sr, is 0.31. The approximate reduction factor to the building, as above, is therefore

$$\frac{4\pi}{4.44} \times \frac{1}{32^2} \times 0.31 \approx 10^{-3}$$

The 90 mrem is reduced to about 0.1 mrem which itself is well below the 10 mrem criteria. If more sophisticated estimates of dose equivalent emerging from vent openings is required, MCNP calculations might be pursued.

VI.B Vent on Opposite Berm Side

As indicated on Fig. 1, a vent also exists on the berm on the tunnel side opposite Bldg. 1005. This vent is Gollon's V-22. The actual second leg is somewhat longer than assumed by Gollon. In exactly the same manner as immediately above, Gollon's result of 235 mrem which corresponds to a second leg length of 1.98 scales to 184 mrem at the survey indicated depth, 8 ft., which corresponds to $d = 2.25$ in a 4 ft. diameter pipe. Although the sidewise reduction factor of 10 may be an overestimate here, due to the small length of the last leg, even a very modest factor reduces this contribution to less than the 160 mrem criteria.

VI.C Access Labyrinth

The main access labyrinth, which has a punch through problem discussed in section IV (B) [2] above, is quite good as a labyrinth. This is labyrinth P-8 in Ref [14]. The estimate there, which is calculated at the point where the third leg tunnel goes under the building, is 1.85 mrem; a clearly negligible contribution.

VI.D Escape Shaft

The escape shaft is labyrinth P-19 in Ref. [14]. The result is 45.5 mrem evaluated at the position where the last leg exits the berm. A person standing to the side of the escape shaft enclosure would nominally receive 1/10 of this dose. The cinder block enclosure extends another 10 ft. beyond this point. Applying the Goebel attenuation factor given above to this 6 ft. × 8 ft. shaft obtains a reduction factor of 20, which means that the estimate of the dose to a person standing at the end of the shaft is about 2 mrem. Although these numbers are inconsequential, the region just northeast of the escape shaft exit has very thin shielding as discussed in Section IV.B.1 above.

VI.E Cryogenics Penetration

The cryogenic return line, as has been mentioned previously, is a small (4.5" dia.), long (14 ft.) straight penetration whose position is shown in Fig. 3. The estimate here is composed of two parts: (1) An entrance dose reduced by the first labyrinth leg formula of Goebel which is used by Gollon¹⁴ in the multi-leg evaluations, and (2) an estimate of punch-through which is described elsewhere.¹⁶

The first leg attenuation formula is the following:

$$H = \frac{1}{1 + 2.5\sqrt{d} + 0.17d^{1.7} + 0.79d^3}$$

As in the earlier expression, d is the length of the leg in units of the square root of the area. In this case, d is very large — 42.1 — which gives a very small attenuation factor, 1.7×10^{-5} . As should be clear from inspection of Fig. 3, the entrance dose geometry is quite complicated. It is taken to be the following:

$$H_0 = \frac{6.6 \times 10^{-6}}{6.25^2} \text{ stars/cc} / p \times \frac{1}{1.8} \times .85 \times 2.4 \times 10^{-2} \text{ mrem/star/cc} \times 1.14 \times 10^{13} p$$

Here, the initial term is the star density from Section III evaluated at $d = 0$ — which should be conservative, the 1.8 factor is the reduction discussed in Section IV.B.1 above due to the finite length of the alcove, and the .85 follows Gollon's procedure of taking 85% of the maximum CASIM dose as the appropriate fraction for labyrinth attenuation. The remaining two terms are simply the usual star density to dose equivalent conversion and half the number of protons at 4 times the design intensity. The H value turns out to be about 22 rem which is reduced to about **0.4 mrem** by the very small value of H given above.

The punch-through was estimated with the "DOSEXIT" program described in Ref. [16]. The result multiplied¹⁷ by 2 is **approximately 10 mrem**.

These estimates must be considered highly uncertain, because it is not clear that either labyrinth formula or the punch-through estimation procedure are at all reliable for holes of this small size. However, the facts that the nominal estimates are small and that this region is part of the berm to which shielding must be added, as recommended below, at least gives no cause for concern.

VII. Skyshine

The Collider Center is subject to "illumination" by skyshine from sources which suffer chronic beam loss. The closest such source is the injection septum¹⁸, where a 0.5% loss has been assumed.² This magnet is about 510 ft (155.4m) from the closest point of Building 1005.

The skyshine estimate is made by using the fit to data obtained at the AGS by Distenfeld and Colvett.¹⁹ The parameterization is the following:

$$\text{Dose in rem / neutron} > 20 \text{ MeV} = \frac{8.33 \times 10^{-13} \times e^{-D/600} \times (1 - e^{-D/47})}{D^2}$$

where D is the distance from the source in meters. For the case of the injection septum, D = 155.4m and the yearly dose at Bldg. 1005 becomes:

$$\text{Dose (rem/year)} = 2.5 \times 10^{-17} \times (\text{No. neutrons} > 20 \text{ MeV emerging from berm per year})$$

The number of neutrons emerging from the berm per 28 GeV/c proton interacting in the septum can be estimated by first approximating the berm by a simple shell of earth of thickness d extending to a transverse radius R from the primary source. The number of neutrons per interacting proton is then roughly:

$$\text{Neut} > 20 \text{ MeV} / p = \left(\frac{\pi}{2} \times R\right) \times 1.44 \times \lambda \times \int_z SD(z) dz$$

The explanation of this expression is as follows. SD is the CASIM star density at the outer berm radius R and some point in the beam direction z . λ is the high energy (>50 MeV) neutron interaction length which is 53.3 cm in BNL soil. The quantity $\lambda \times SD$ is the flux (neutrons per cm^2) at R, z above the CASIM threshold of 50 MeV and the 1.44 factor corrects this to the flux above 20 MeV. An area on the berm surface of $dA = (\pi/2) \times R \times dz$ corresponds to considering a vertical half angle of $\pm 45^\circ$ to be the radiating surface. The integral over the beam direction then gets the total neutrons.

We rely on some 28 GeV/c CASIM calculations that were done as a part of the transfer line shielding estimation for numerical values. The maximum Star Density in earth was well described by the following:

$$R^2 \times SD_{\max}(28 \text{ GeV}) = 1.2 \times 10^{-6} \times e^{-d/1.67}$$

and the integral over the beam direction by $\int SD dz = 693 \times SD_{\max}$

The transverse shielding in the region of the septum is well represented by an R value of 6.98m and a d value of 13 ft. = 3.96m. Plugging in all the numbers gives

$$\text{Neut} > 20 \text{ MeV} / p = 3.9 \times 10^{-3}$$

Combining this with the dose per year given above gives,

$$\text{rem/year} \cong 10^{-19} \times \text{No. interacting protons per year.}$$

Now the number of equivalent 28 GeV/c protons per ring per year is given by the Beam Loss Scenario (at 4 times the design intensity) as about 5.2×10^{16} so a 0.5% loss is 2.6×10^{14} protons, which gives a total estimated skyshine on Bldg. 1005 of .026 mrem per year.

VIII. Recommendations

In order to meet the stringent criteria adopted for faults, the berm in two regions, as indicated in Figs. 5 and 9, must be increased. Fig. 14 shows a sketch indicating the area affected by the increased berm. The patched area on the right hand side of Fig. 14, whose cross section is shown in Fig. 5, basically extends the existing berm contours at the position where the maximum elevation is 95 ft. a distance of 100 ft. in the northeast direction. After 100 feet, the raised berm can be smoothed into the existing berm. The vent outlet in the region of the added berm must be raised. The patched area on the left of Fig. 14 is the region whose cross section is Fig. 9. A maximum of about 3 ft. of vertical cover is needed (see Fig. 9) extending from the right hand side of the escape exit in Fig. 14 for a distance of 50 ft. To the left of the escape exit and to the right after a 50 ft. distance, the added berm can be graded into the existing berm.

In addition, a concrete block nominally 3 ft thick should be placed at the end of the first leg of the main access labyrinth. It's width should be the width of this leg and the height should extend as close as possible to the ceiling height.

References/Footnotes

1. The definition of "high occupancy" is 2000 hrs/yr. Any location whose occupancy is expected to be greater than 1/2 hr. per day for extended periods of time will be treated as a high occupancy region. Low occupancy regions are therefore those which are expected to be inhabited less than 125 (2000/16) hrs per year by a specific individual.
2. M. Harrison and A.J. Stevens, "Beam Loss Scenario in RHIC," AD/RHIC/RD-52 (1993). The design basis fault is loss of the full beam on any magnet which is close to being a machine aperture and loss of half the beam on other magnets. The only magnets near the collider center are those of the regular lattice which are not machine apertures. As discussed in this reference, the occurrence of such faults should be far less than once per year.
3. Aerial survey of April 3, 1991 prepared by Chas. H. Sells, Inc. The aerial survey map shows 2 ft. elevation contours.
4. "Conceptual Design of the Relativistic Heavy Ion Collider," BNL52195, pp. 259-261 (1989). See also P.J. Gollon and W.R. Casey, "ISABELLE Shielding Criteria and Design," Health Phys. 46, pp. 123-131 (1984).

5. A. Van Ginneken, "CASIM; Program to Simulate Hadron Cascades in Bulk Mater," Fermilab FN-272 (1975). For the modifications to CASIM for heavy ion transport see A.J. Stevens, "Maximum Energy Deposition Densities in the Internal Dump." AD/RHIC/RD-41 (1992).
6. If the transverse azimuth is divided into 4 sections — up, down, left, and right — the up,down is typically reduced by 5-15%, and the left, right enhanced by the same amount. Magnetic field effects are much larger near the loss point.
7. The errors in Fig. 4 are simply the statistical errors derived from computer runs with different random number seeds. The "data points" for the proton runs represent the average of 6 runs with 100000 primaries each. For Au, three runs were made, each with 25000 primaries. CASIM is an order of magnitude slower per primary for Au ions than for protons.
8. If there were no difference between Au ions and protons, the Au star density multiplied by $(250/100)^{0.8}$ and divided by 197 should "lie on top of" the proton points. This factor is .0105 whereas .01 was used in Fig. 4.
9. U.S. Department of Energy Radiological Control Manual, DOE/EH-0256T (1992).
10. The zero transverse distance in Fig. 7 is the magnet beam line, not the tunnel center line.
11. Dejan Trbojevic, private communication.
12. Dejan Trbojevic, private communication. The actual expectation is 90% H and 10% He with other gases being "frozen out." In the cross section estimations and the CASIM calculation we assume the beam interacts with a nucleus having an atomic weight of 1.1.
13. For Au, the geometric cross section was used, which is 1.475 bn for Au on H.
14. P.J. Gollon, "Shielding of Multi-Leg Penetrations into the RHIC Collider," AD/RHIC/RD-76 (1994).
15. H.G. Vogt, "Monte Carlo Calculations of the Neutron Transmission Through the Access Ways of the CERN Super Proton Synchrotron," CERN 75-14 (1975).
16. A.J. Stevens, "An Approximate Method for Evaluating Neutron Punch Through in Certain Classes of Shielding Penetrations," AD/RHIC/RD-65 (1994).
17. The method described in Ref [16] above underestimates measured values by a factor of 2. This method can also be used to estimate punch-through from the walls of the last legs of multi-legged labyrinths. The estimates were made for those labyrinths discussed in the text and found to be typically 10% or less of the dose from labyrinth attenuation.
18. The other chronic sources are collimators and beam dumps which are much further away. The small result for the source considered justifies ignoring other sources.

19. C. Distenfeld and R. Colvett, "Skyshine Considerations for Accelerator Shielding Design," Nucl. Sci. Eng. Vol. 26, p. 117 (1966). The expression given in this reference has been multiplied by 2 because skyshine is dominated by low energy neutrons and we are assuming double the current quality factor.

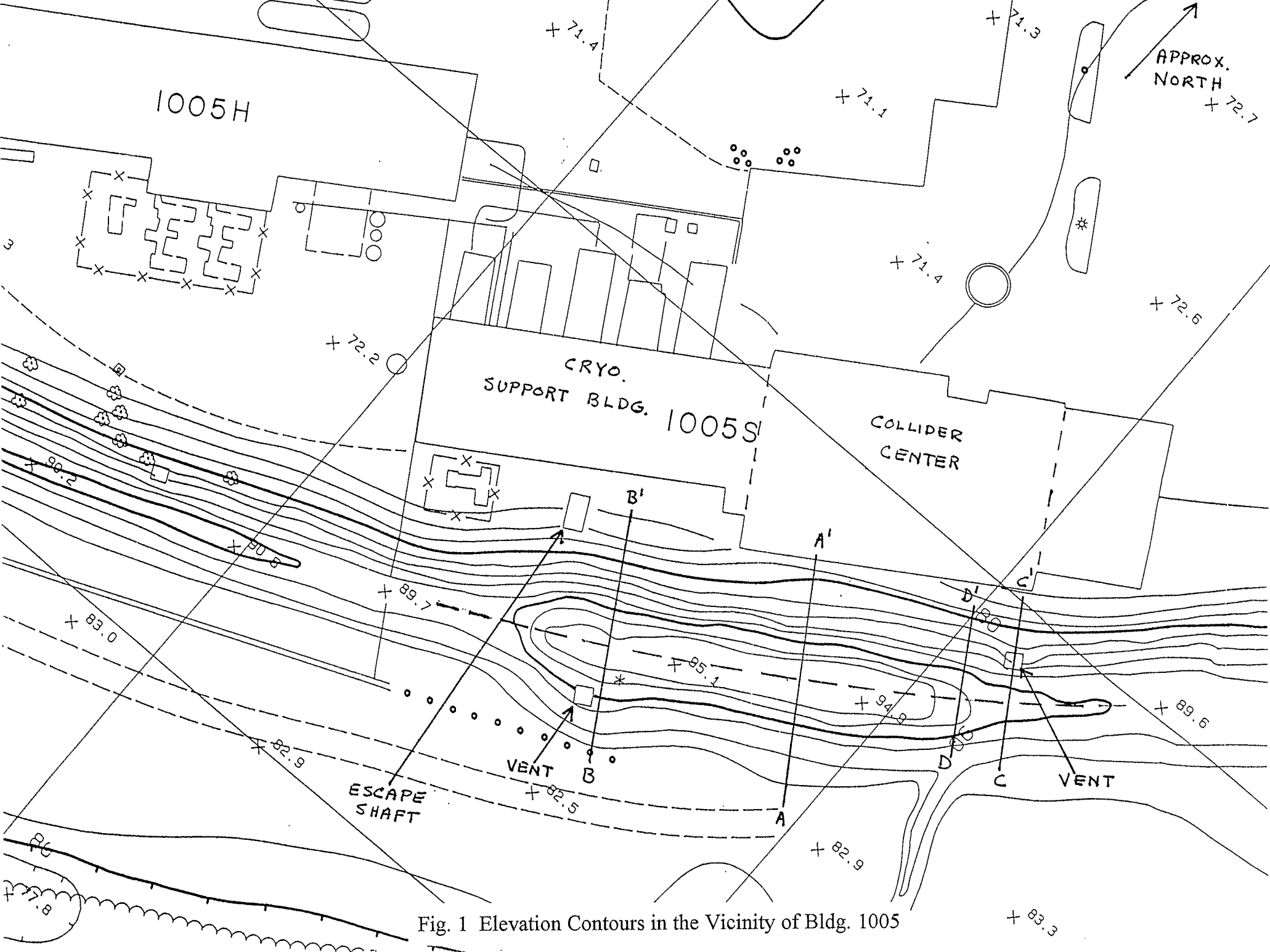


Fig. 1 Elevation Contours in the Vicinity of Bldg. 1005

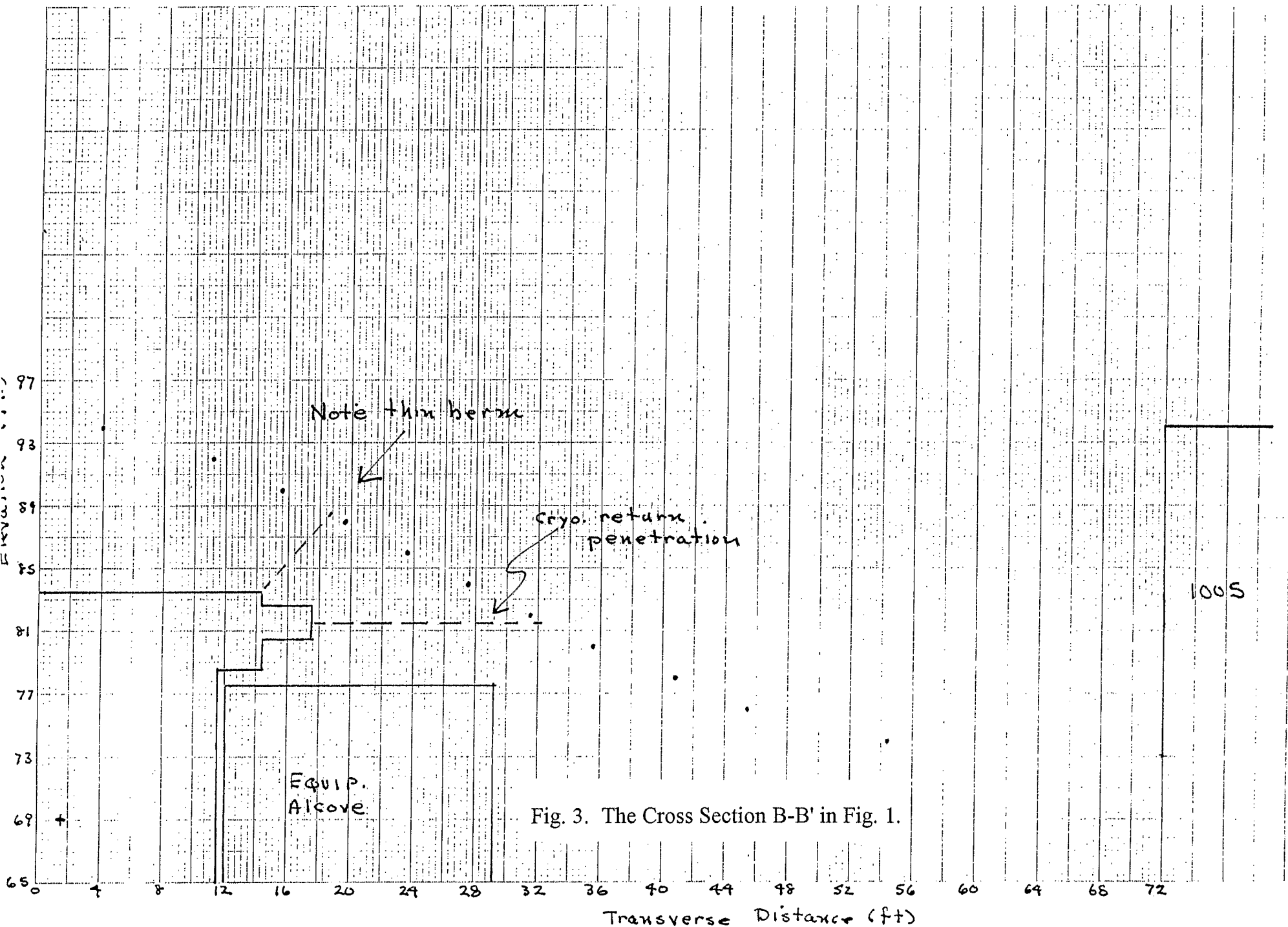
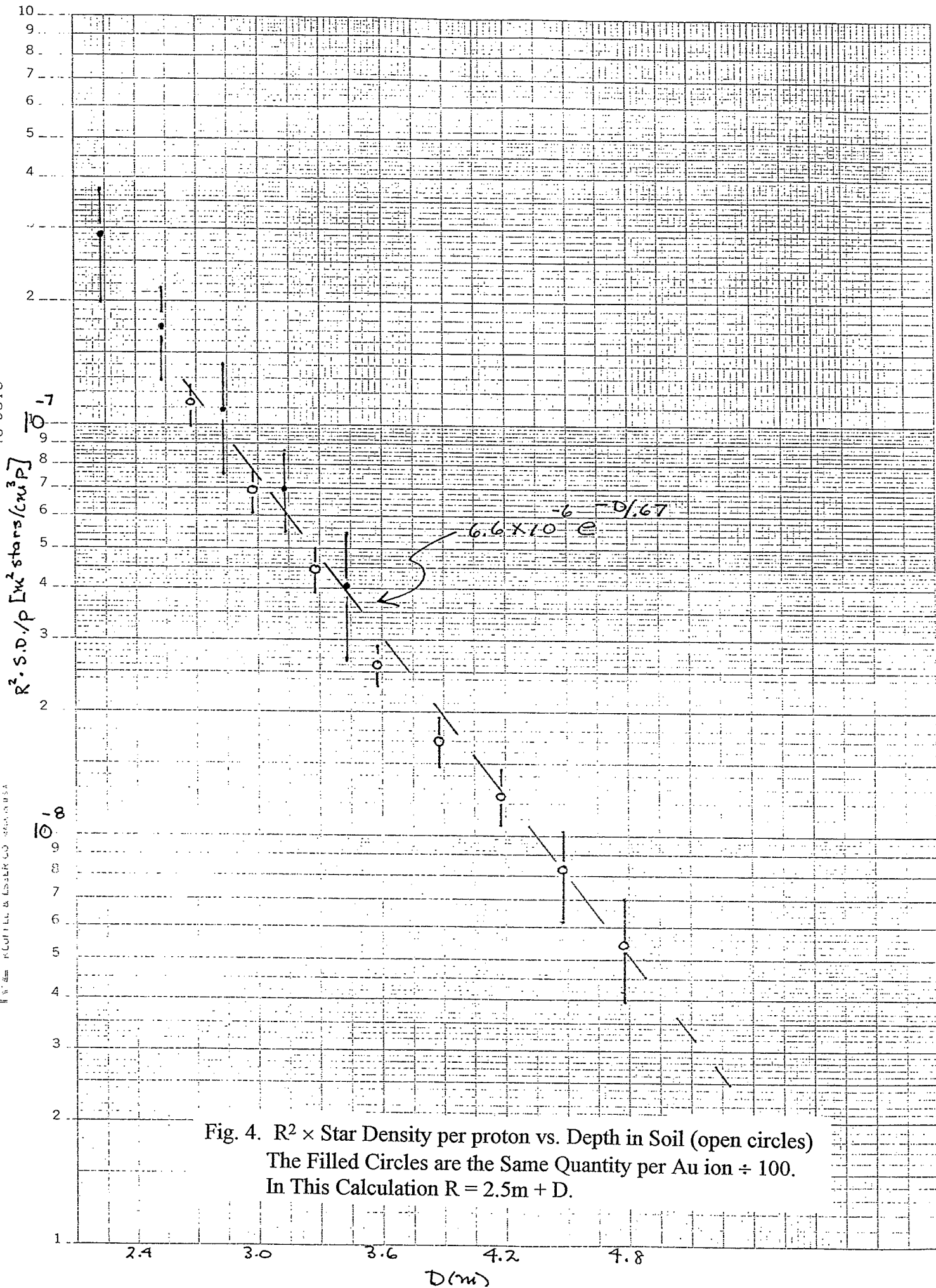


Fig. 3. The Cross Section B-B' in Fig. 1.



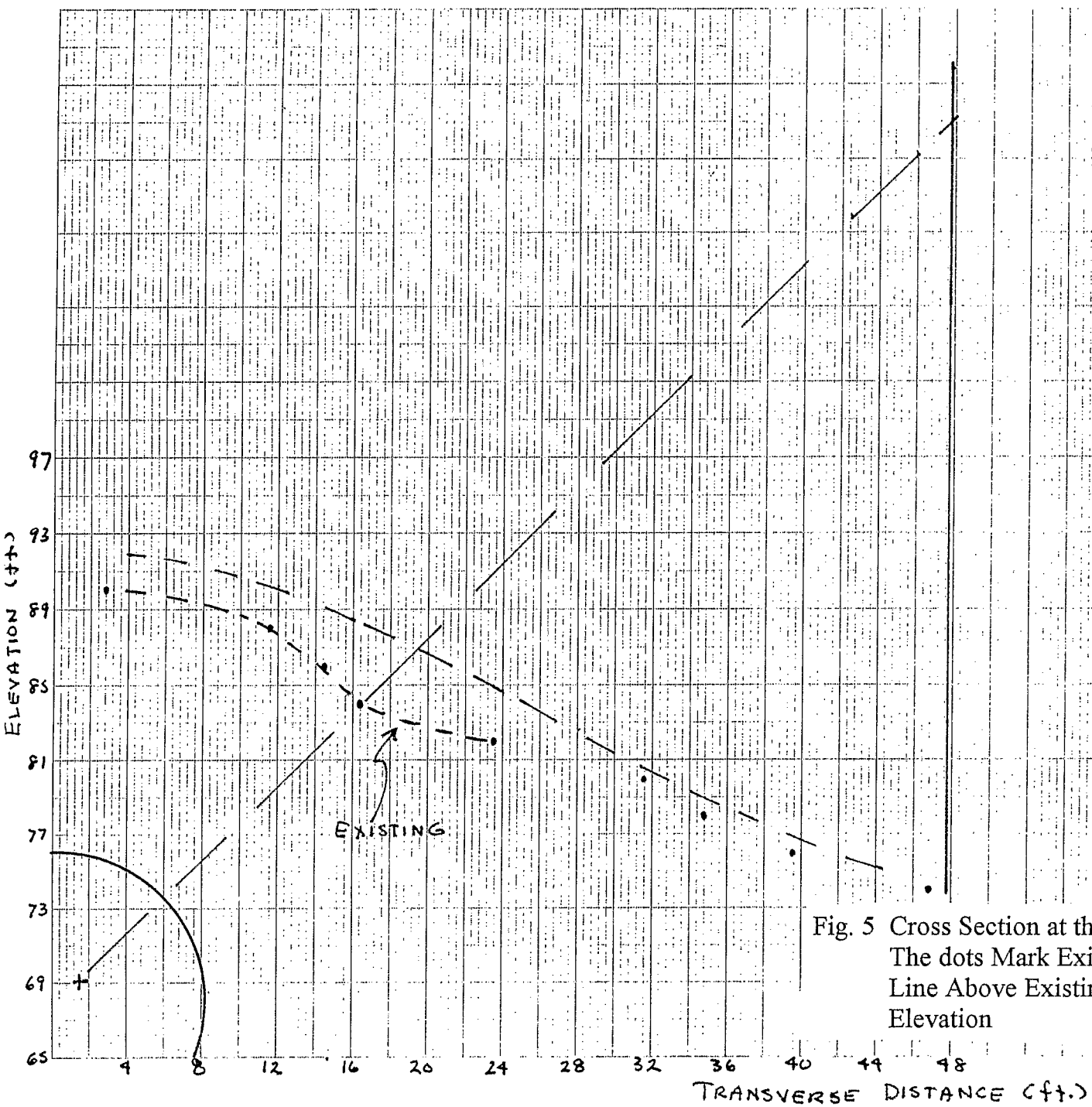


Fig. 5 Cross Section at the Building Corner Near C' in Fig. 1
 The dots Mark Existing Elevation. The Higher Dashed
 Line Above Existing Elevation Basically Extends the A-A'
 Elevation

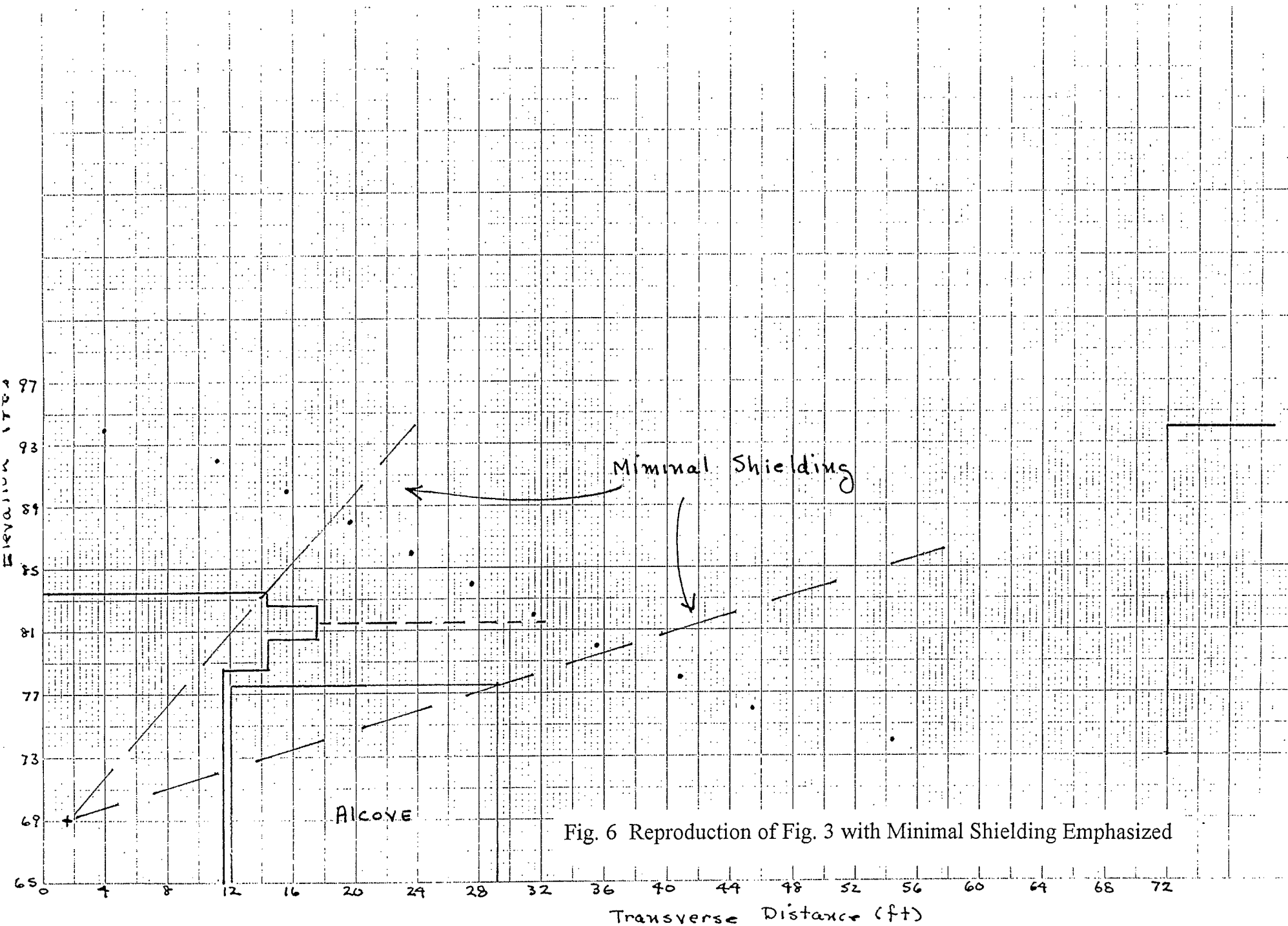


Fig. 6 Reproduction of Fig. 3 with Minimal Shielding Emphasized

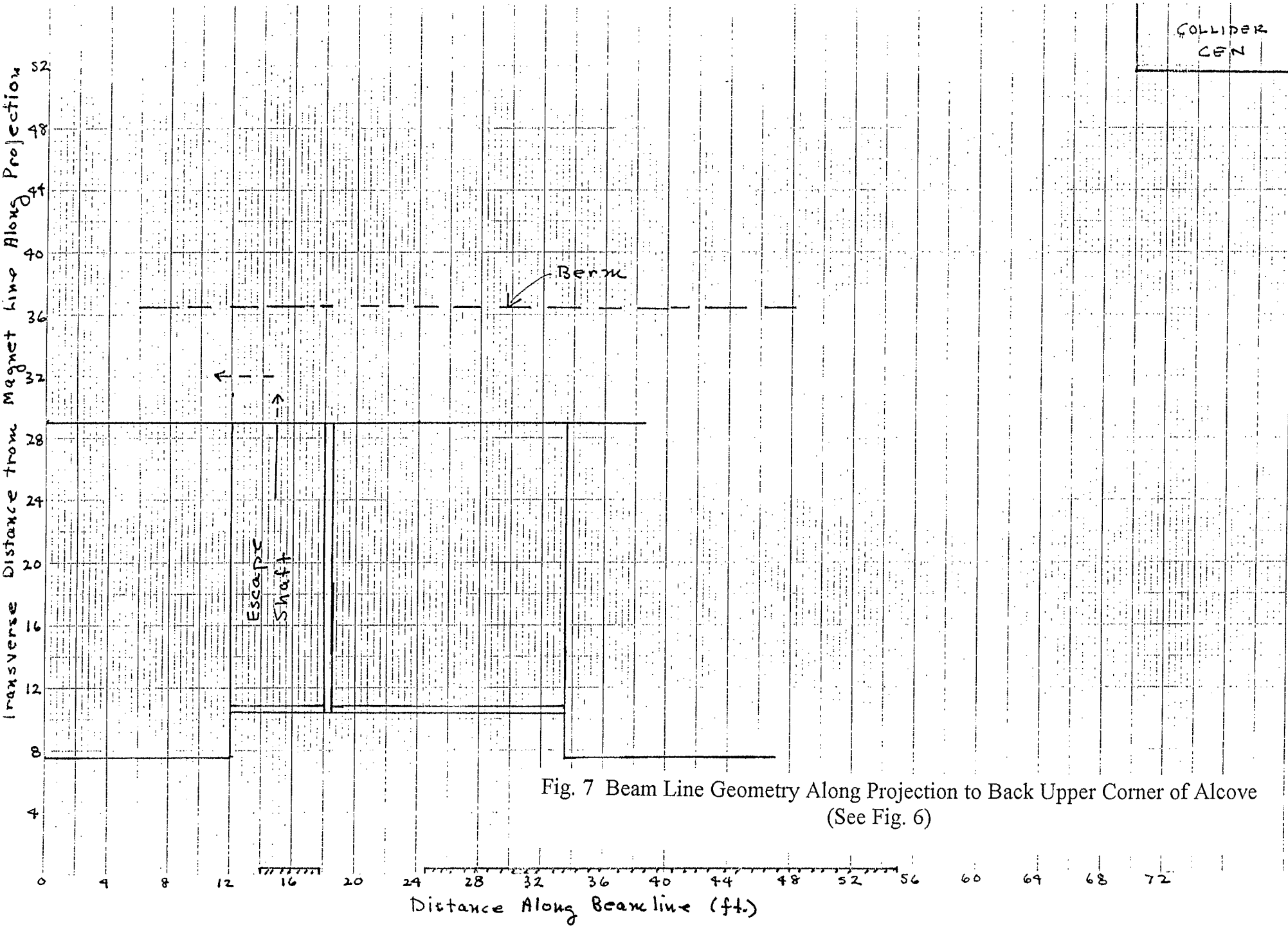


Fig. 7 Beam Line Geometry Along Projection to Back Upper Corner of Alcove
(See Fig. 6)

40 5010
new p

KEUFFEL & ESSER CO. MADE IN U.S.A.

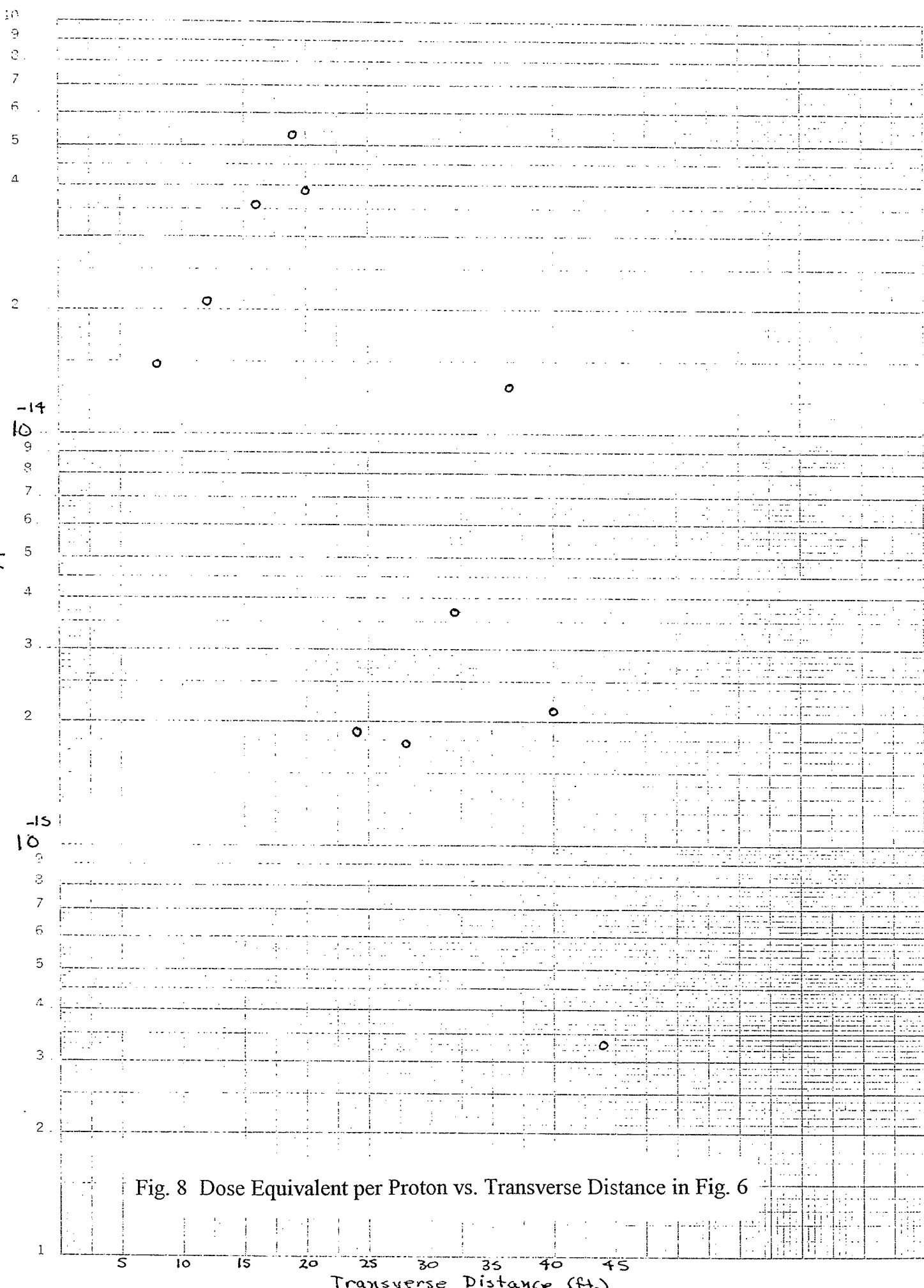


Fig. 8 Dose Equivalent per Proton vs. Transverse Distance in Fig. 6

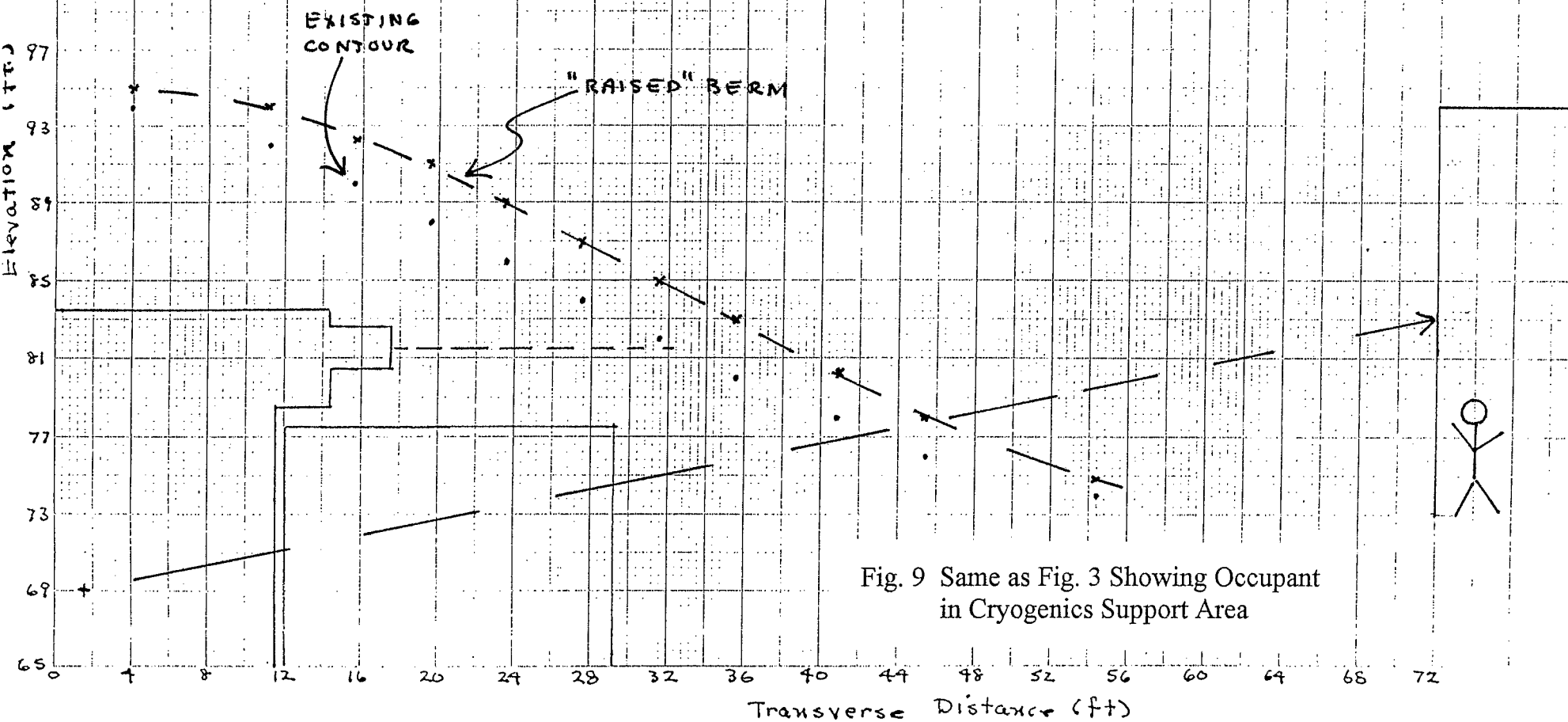


Fig. 9 Same as Fig. 3 Showing Occupant
in Cryogenics Support Area

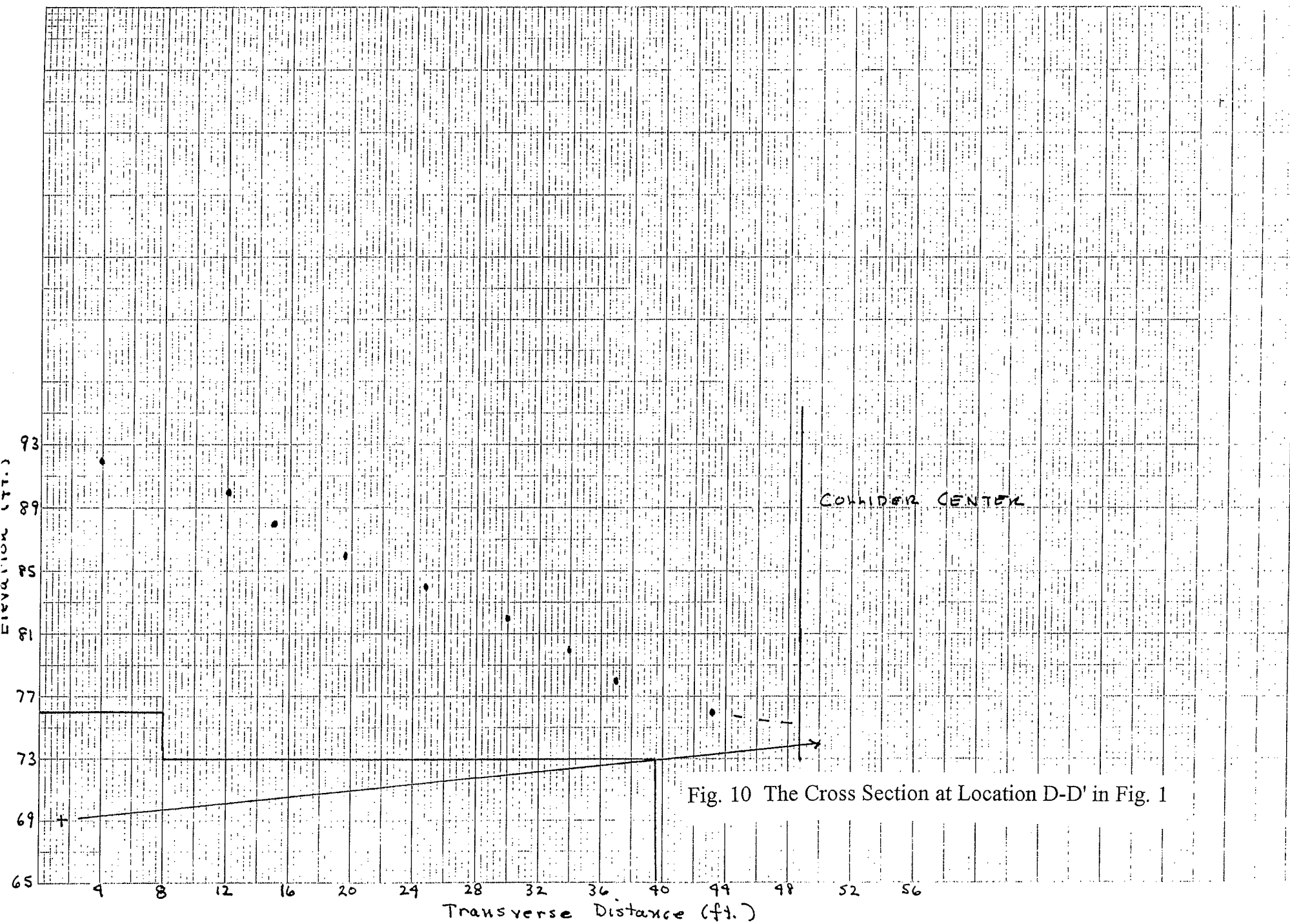


Fig. 10 The Cross Section at Location D-D' in Fig. 1

46 6210

Stars/cm³ pSEMI-LOGARTHERMIC 5 CYCLES X 10 DIVISIONS
KEUFFEL & ESSER CO. MADE IN U.S.A.10⁻¹⁰10⁻¹¹10⁻¹²

250 GeV protons
on $\langle A \rangle = 1.1$
Interactions forced
to occur at $z=0$

Fig. 11 Star Density (Smoothed) in Soil vs. Z (Beam Direction)
in Tunnel Geometry at R=6.225m, d=3.725m

7.5

15.0

22.5

Z (m)

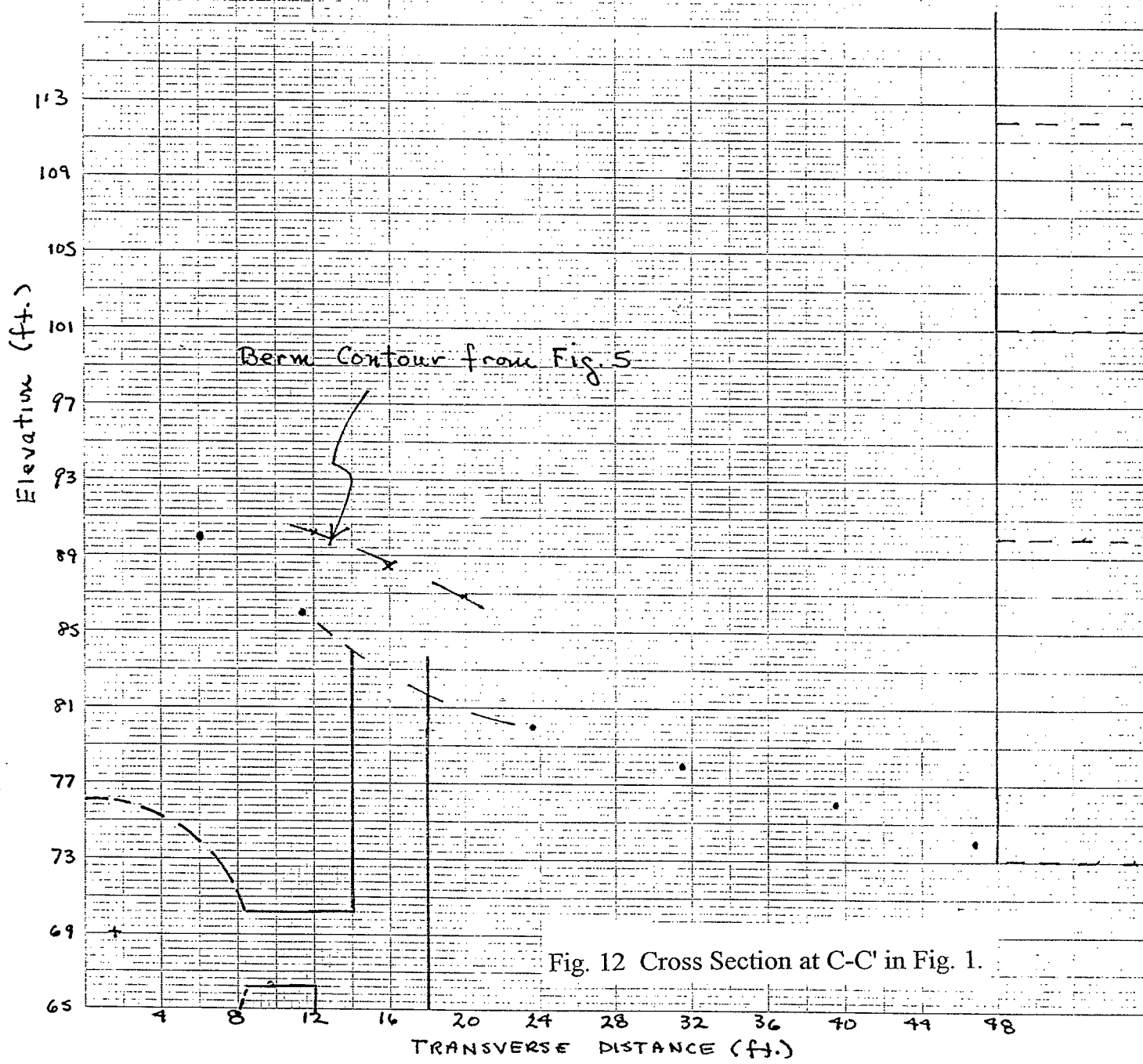


Fig. 12 Cross Section at C-C' in Fig. 1.

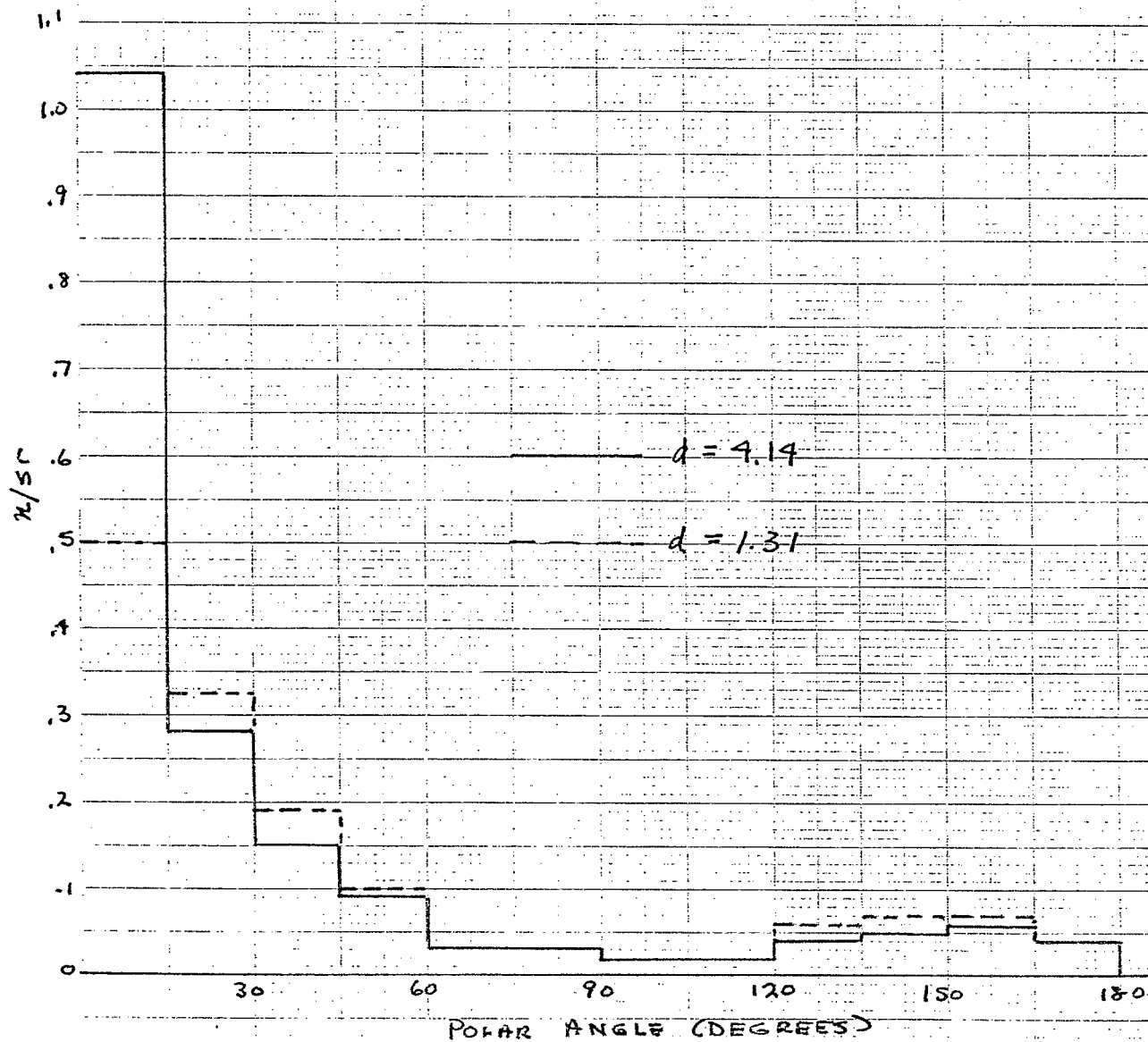


Fig. 13 Neutron Direction vs. Universal Length
Adapted from Fig. 9 of Ref. [15]

